



## Molecular Crystals and Liquid Crystals Science and Technology. Section A. Molecular Crystals and Liquid Crystals

Publication details, including instructions for authors and subscription information:

<http://www.tandfonline.com/loi/gmcl19>

### On the Peculiar Macromolecular Organization of Nematic Poly(Urethane- Ester)S

O. Francescangeli <sup>a</sup>, M. Laus <sup>b</sup> & G. Galli <sup>c</sup>

<sup>a</sup> Dipartimento di Scienze dei Materiali a della Terra, and Istituto Nazionale per la Fisica della Materia Università di Ancona, Via Brecce Bianche, 60131, Ancona, Italy

<sup>b</sup> Dipartimento di Chimica Industriale a dei Materiali Università di Bologna, Viale Risorgimento 4, 40136, Bologna, Italy

<sup>c</sup> Dipartimento di Chimica a Chimica, Industriale Università di Pisa, Via Risorgimento 35, 56126, Pisa, Italy

Version of record first published: 04 Oct 2006

To cite this article: O. Francescangeli, M. Laus & G. Galli (1997): On the Peculiar Macromolecular Organization of Nematic Poly(Urethane-Ester)S, Molecular Crystals and Liquid Crystals Science and Technology. Section A. Molecular Crystals and Liquid Crystals, 299:1, 407-417

To link to this article: <http://dx.doi.org/10.1080/10587259708042021>

PLEASE SCROLL DOWN FOR ARTICLE

Full terms and conditions of use: <http://www.tandfonline.com/page/terms-and-conditions>

This article may be used for research, teaching, and private study purposes. Any substantial or systematic reproduction, redistribution, reselling, loan, sub-licensing, systematic supply, or distribution in any form to anyone is expressly forbidden.

The publisher does not give any warranty express or implied or make any representation that the contents will be complete or accurate or up to date. The accuracy of any instructions, formulae, and drug doses should be independently verified with primary sources. The publisher shall not be liable for any loss, actions, claims, proceedings, demand, or costs or damages whatsoever or howsoever caused arising directly or indirectly in connection with or arising out of the use of this material.

## ON THE PECULIAR MACROMOLECULAR ORGANIZATION OF NEMATIC POLY(URETHANE-ESTER)S

ORIANO FRANCESCANGELI<sup>1</sup>, MICHELE LAUS<sup>2</sup>, GIANCARLO GALLI<sup>3</sup>

<sup>1</sup>Dipartimento di Scienze dei Materiali e della Terra, and Istituto Nazionale per la Fisica della Materia

Università di Ancona, Via Brecce Bianche, 60131 Ancona, Italy

<sup>2</sup>Dipartimento di Chimica Industriale e dei Materiali

Università di Bologna, Viale Risorgimento 4, 40136 Bologna, Italy

<sup>3</sup>Dipartimento di Chimica e Chimica Industriale

Università di Pisa, Via Risorgimento 35, 56126 Pisa, Italy

**Abstract** The peculiar mesophase structure of a series of thermotropic poly(urethane-ester)s is discussed. The polymers form different nematic phases, namely a nematic mesophase with cybotactic groups and a conventional nematic mesophase. The X-ray diffraction analysis suggests that two types of structural arrangements, namely smectic C-like and conventional nematic structures, coexist inside the cybotactic nematic mesophases, to which different internal degrees of correlation correspond. The correlation length parallel to the director of the nematic mesophase ranges from 38 to 45 Å. In the cybotactic groups the correlation lengths parallel and perpendicular to the director range from 260 to 560 Å and 130 to 270 Å, respectively.

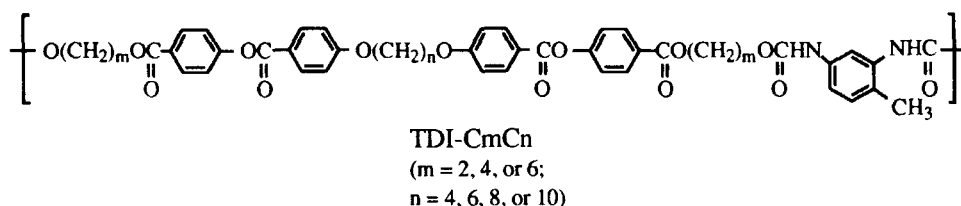
### INTRODUCTION

The detailed analysis of the thermodynamic behavior of nematic polymers and its correlation with a variety of structural features, including the mesogenic group, flexible spacer and linking group, has allowed the macroscopic and microscopic ordering of the macromolecules to be predicted to some extent. Comparatively little information is

available about the role of hydrogen bonding interactions in affecting the mesophase behavior of polymers, namely thermoplastic polyurethanes. In these materials, in fact, the synthetic control of the micro- and macro-architectural parameters is definitely more difficult than the one for polyesters with analogous structure<sup>1-5</sup>. In addition, they usually show high melting temperatures and moderate thermal stability.

However, the systematic study of these polymers can help address the fundamental question whether hydrogen bonding will enhance, or otherwise depress the propensity of the polymers to give rise to stable mesophases, and how mesophase transition and ordering will be driven by the formation/destruction of such intermolecular interactions in condensed states.

Within this general scope, a series of papers<sup>6-8</sup> has recently been devoted to the study of the mesomorphic behavior of semiflexible poly(urethane-ester)s TDI-CmCn with the following structure:



It was found that several of the above poly(urethane-ester)s formed a nematic mesophase with cybotactic groups followed by a conventional nematic mesophase at higher temperature<sup>7</sup>. In the present paper we will reconsider their LC behavior and mesophase structure with the aim of providing a detailed description of the peculiar macromolecular organization in the *cybotactic* nematic mesophase as revealed by X-ray diffraction analysis of oriented fiber specimens.

## EXPERIMENTAL PART

Poly(urethane-ester)s TDI-CmCn were prepared from mesogenic alkylene di[4-( $\omega$ -hydroxyalkoxy-4-oxybenzoyl)oxybenzoate]s (CmCn) and 2,4-toluenediisocyanate (TDI), as described elsewhere<sup>6</sup>. X-ray diffraction photographs on oriented samples were taken by means of a conventional X-ray powder diffractometer equipped with a pin-hole flat-plate camera with a temperature controlled cell ( $\pm 0.1$  °C). Ni-filtered CuK $\alpha$  radiation ( $\lambda = 1.54$  Å) was used. Fibers were oriented by pulling up with tweezers the viscous

liquid crystal melt at different temperatures throughout the entire mesophase range, or the isotropic melt. Intensity contour maps were obtained by digitalizing the X-ray diffraction patterns, using the Kodak photo-CD system, and elaborating by Spyglass Transform image processing program.

## RESULTS AND DISCUSSION

Polymers TDI-C6C4, TDI-C6C10 and TDI-C2C6 form one mesophase, while polymers TDI-C6C8, TDI-C6C6 and TDI-C4C6 give rise to two sequential mesophases. However, X-ray diffraction studies on powder samples had previously shown the mesophase to be nematic throughout the entire mesomorphic range for each polymer<sup>7</sup>. More detailed information was obtained from the oriented mesophases produced by drawing fibers at different temperatures<sup>8</sup>. The X-ray diffraction spectra of the oriented samples TDI-C6C4, TDI-C6C10 and TDI-C2C6 were nearly identical to those of TDI-C6C8, TDI-C6C6 and TDI-C4C6 that had been oriented at temperatures within the existence range of the lower temperature mesophase. As typical examples, the fiber patterns of samples TDI-C6C4 and TDI-C6C10 are reported in Figure 1.

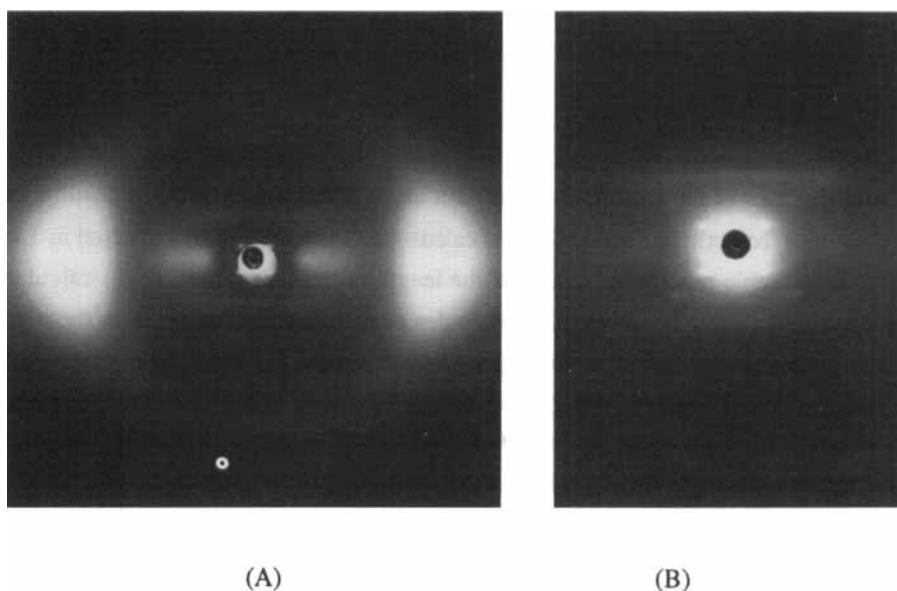


FIGURE 1. X-ray diffraction patterns of the oriented mesophase of polymer (A) TDI-C6C4 (vertical fiber axis; sample to film distance 75 mm) and (B) TDI-C6C10 (small-angle region; sample to film distance 145 mm).

The diffraction pattern consists of two symmetrically placed wide-angle broad crescents centered on the equator, due to the liquid-like short-range order of the mesogenic groups (average distance  $D \approx 4.7$  Å), and four sharp small-angle spots symmetrically placed about the direct beam and forming pairs on a straight line at an angle  $\beta$  with respect to the meridian, i.e. the fiber axis. The second harmonics of the small-angle spots are also detected in the diffraction patterns of sample TDI-C6C10. In addition, a small fraction of the scattered intensity is localized on regularly spaced diffuse lines situated in the direction perpendicular to the fiber axis. The above X-ray spectra are very similar to those reported for other liquid crystalline polymers<sup>9,10</sup>, and point to the presence of a nematic mesophase with cybotactic smectic C-like groups<sup>11</sup>. The relevant X-ray data are summarized in Table I.

TABLE I X-ray diffraction data of polymers TDI-CmCn.  
( $\beta$  and  $d$  are the tilt angle and the layer spacing, respectively).

Sample	$\beta$ (deg)	$d$ (Å)	$L_{\text{exp}}$ (Å)	$L_{\text{calc}}$ (Å)
TDI-C6C4	49.0	36.4	55.5	55.0
TDI-C6C6	46.4	39.4	57.1	58.5
TDI-C6C8	50.0	38.5	59.9	61.0
TDI-C6C10	54.2	37.3	63.8	63.5
TDI-C2C6	46.4	32.2	46.7	48.5
TDI-C4C6	49.8	33.5	51.9	53.5

From the values of the spacing  $d$  and the tilt angle  $\beta$  the length of the repeating unit,  $L_{\text{exp}}$ , in the cybotactic nematic phase was calculated. These values are collected in Table I. The same Table reports the values of the length of the repeat unit,  $L_{\text{calc}}$ , calculated from standard atomic bond lengths and angles considering the molecule in the planar fully extended conformation. A good agreement between  $L_{\text{exp}}$  and  $L_{\text{calc}}$  is observed for all samples.  $L_{\text{exp}}$  increases linearly with increasing length of both the flexible spacers. The value of 2.6 Å for the projection of two C-C bonds in the polymethylene chain is in good agreement with the expected value of 2.54 Å in a polymethylene chain<sup>12</sup>. Accordingly, the conformation of the polymethylene spacers does not depart considerably from the fully extended one, independent of their position in the polymer repeat unit.

The regularly spaced diffuse lines perpendicular to the meridian and symmetrically placed above and below the equator are attributed to the coherent diffuse intermolecular

scattering associated with the uncorrelated longitudinal disorder<sup>13,14</sup>. The same type of diffuse streaks was found in the diffraction patterns of both polymeric smectic phases<sup>15,16</sup> and polymeric<sup>17</sup> and low molar mass nematic<sup>18</sup> phases and indicate that the molecules tend to align in rows over a short range. The diffraction pattern for a series of parallel periodic chains with periodicity  $a$  but with a disordered net of chain centers is a series of sheets of scattering normal to the chains and spaced  $1/a$  apart<sup>14</sup>. The correlation length of this ordering process may be estimated from the width of the diffuse streaks along the director<sup>13</sup>. From the measurement of the spacing between adjacent diffuse lines in the reciprocal space it is possible to estimate the period,  $L_{\text{diff}}$ , of the corresponding linear lattice in the real space, which is of the order of the molecular length. The  $L_{\text{diff}}$  values obtained are significantly lower than the corresponding  $L_{\text{calc}}$  values estimated for the most extended molecular conformation. The difference  $L_{\text{calc}} - L_{\text{diff}}$  varies from a minimum of 4 Å for TDI-C6C4 to a maximum of 8 Å for TDI-C6C8 and can be explained as a tilt effect. If we consider the mean projection of the molecular length along the director, i.e.  $d = L \langle \cos \phi \rangle$ , we can calculate an average angle  $\phi$  of the molecule from its preferred direction ( $\phi = 0^\circ$ ). The values of  $\phi$  so obtained are  $22^\circ$ ,  $24^\circ$ ,  $25^\circ$ ,  $26^\circ$ ,  $27^\circ$  and  $29^\circ$  for TDI-C6C4, TDI-C6C10, TDI-C2C6, TDI-C4C6, TDI-C6C6 and TDI-C6C8, respectively. These values are in good agreement with the average tilt angle usually reported in other low molar mass nematics<sup>19</sup>.

The above findings indicate that two structural arrangements, namely smectic C-like and conventional nematic structures, coexist inside the cybotactic nematic mesophase of these polyurethanes. A schematic model of the structural arrangements of the polymer chains in the cybotactic mesophase is reported in Figure 2.

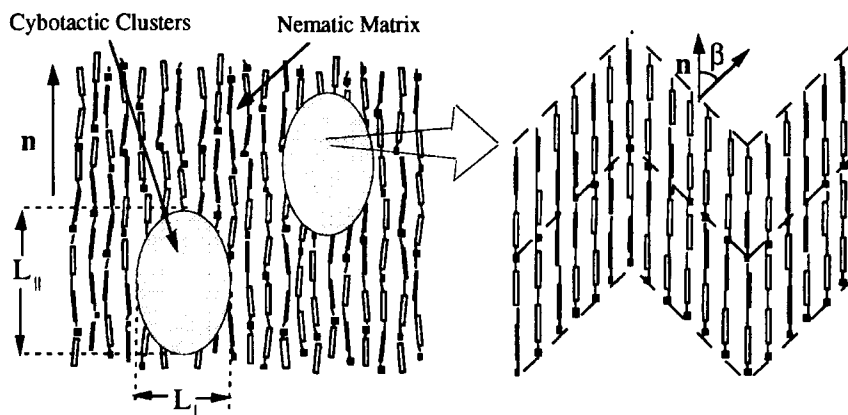


FIGURE 2 Schematic representation of the structural arrangements of the polymer chains in the cybotactic nematic mesophase.

The correlation lengths and the average dimensions of the cybotactic clusters were obtained<sup>8</sup> from the analysis of the intensity profile of the small-angle four-spot pattern in the directions parallel and normal to the director axis  $\mathbf{n}$ . As an example, Figure 3(A) shows the contours of constant intensity of the small-angle region of the diffraction spectrum of TDI-C6C10. The scattered intensity  $I$  as a function of the longitudinal,  $q_{\parallel}$ , and transversal,  $q_{\perp}$ , components of the scattering vector  $\mathbf{q}$  in the reciprocal space (whose modulus is  $q = 4\pi\sin\theta/\lambda$ ,  $2\theta$  being the scattering angle) was measured by performing optical density scans through the maxima of the small-angle spots along the directions parallel and perpendicular to the fiber, respectively, i.e. straight lines  $aa'$  and  $bb'$  of Figure 3(A). Figure 3(B) shows the experimental intensity profiles  $I(q_{\parallel})=I(q_{\parallel}, q_{\perp}=q_{0\perp})$  and  $I(q_{\perp})=I(q_{\parallel}=q_{0\parallel}, q_{\perp})$  about the vector  $\mathbf{q}_0$  of sample TDI-C6C10 (after background subtraction). Similar profiles were obtained for the other poly(urethane-ester)s.

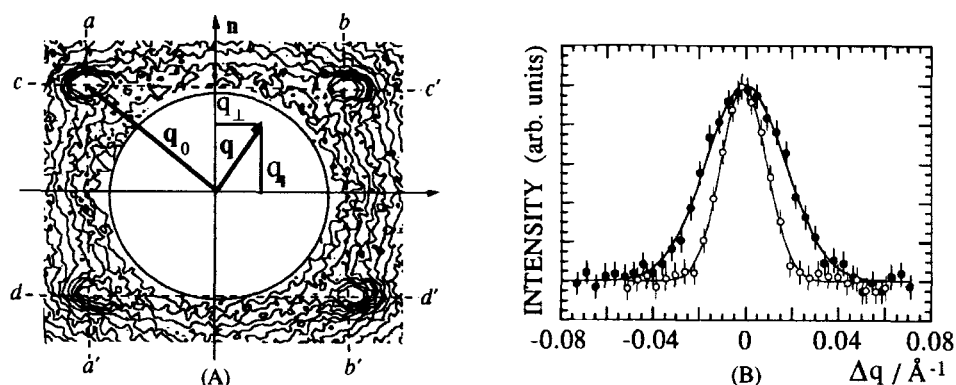


FIGURE 3 (A) Contours of constant intensity of the small-angle region of the diffraction spectrum of sample TDI-C6C10. (B) Longitudinal and transversal intensity profiles of the small-angle diffraction spot of sample TDI-C6C10 measured along the section  $aa'$  (open circles;  $\Delta q = q_{\parallel} - q_{0\parallel}$ ) and  $cc'$  (full circles;  $\Delta q = q_{\perp} - q_{0\perp}$ ), respectively, after background subtraction.  $q_{0\parallel} = 0.0985 \text{ \AA}^{-1}$ ,  $q_{0\perp} = 0.1366 \text{ \AA}^{-1}$ . The continuous lines give the best fit by Gaussian functions.

The best fits of these intensity profiles for all the samples were obtained by using a Gaussian function described by Equation (1)

$$I(q_{\parallel}, q_{\perp}) = I_0 \exp \left\{ - \left[ \frac{(q_{\parallel} - q_{0\parallel})^2}{2 \Delta q_{\parallel}^2} + \frac{(q_{\perp} - q_{0\perp})^2}{2 \Delta q_{\perp}^2} \right] \right\} \quad (1)$$

The Fourier inversion of these diffracted intensity profiles, after correction for the

resolution of the experimental apparatus, allowed to obtain the correlation functions  $G_{\parallel}$  and  $G_{\perp}$  parallel and normal, respectively, to the director in the real space

$$G_{\parallel}(z) = \exp\left(-\frac{z^2}{\xi_{\parallel}^2}\right), \quad G_{\perp}(r) = \exp\left(-\frac{r^2}{\xi_{\perp}^2}\right) \quad (2)$$

where  $z$  and  $r$  are the distances in the real space parallel and perpendicular to the director, respectively, and  $\xi_{\parallel}$  and  $\xi_{\perp}$  are the longitudinal and the transversal correlation lengths, respectively. The trend of the correlation lengths  $\xi_{\parallel}$  and  $\xi_{\perp}$  as a function of the overall number  $N$  of methylene groups in the repeat unit ( $N=2m+n$ ) is reported in Figure 4. A regular increase in  $\xi_{\parallel}$  with increasing  $N$  is observed, whereas  $\xi_{\perp}$  initially increases with  $N$  and then reaches a constant value of about 90 Å. The increase in  $\xi_{\parallel}$  with increasing length of the flexible spacer clearly indicates an effective participation of the flexible spacer in the ordering process.

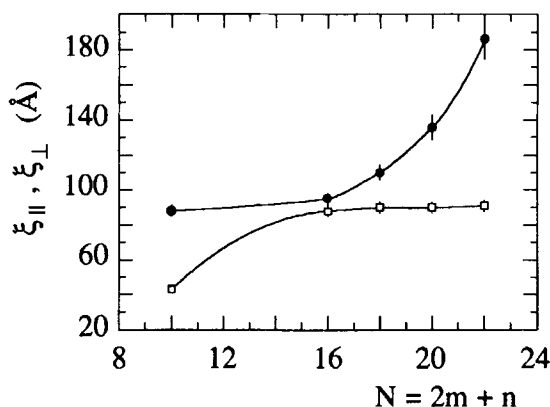


FIGURE 4 Trend of the correlation lengths  $\xi_{\parallel}$  (full circles) and  $\xi_{\perp}$  (open squares) as a function of the number  $N$  of methylene groups in the repeat unit.

Further information about the ordering in the nematic region can be obtained from the analysis of the diffuse scattering in the small-angle region associated with the uncorrelated longitudinal disorder. These diffuse streaks correspond to the intersection with the Ewald sphere of a series of equidistant diffuse planes representing the Fourier transform of a linear modulated object oriented along the director<sup>13</sup> (Figure 5).

From the intensity profile of the diffuse reflections along the director it is possible to estimate the longitudinal correlation length  $\xi_{\parallel}$  in the nematic phase by the equation



$$\xi_{\parallel} = \frac{2}{\Delta q_{\parallel}} \quad (3)$$

where  $\Delta q_{\parallel}$  is the full width at half maximum of the Lorentzian curves describing the shape of the diffuse reflections in the reciprocal space<sup>8</sup>. The values of  $\xi_{\parallel}$  obtained after correction for the finite experimental resolution and averaging over the whole set of diffuse reflections are 38, 40, 42, 42 and 45 Å for samples TDI-C2C6, TDI-C6C4, TDI-C6C6, TDI-C6C8 and TDI-C6C10, respectively.

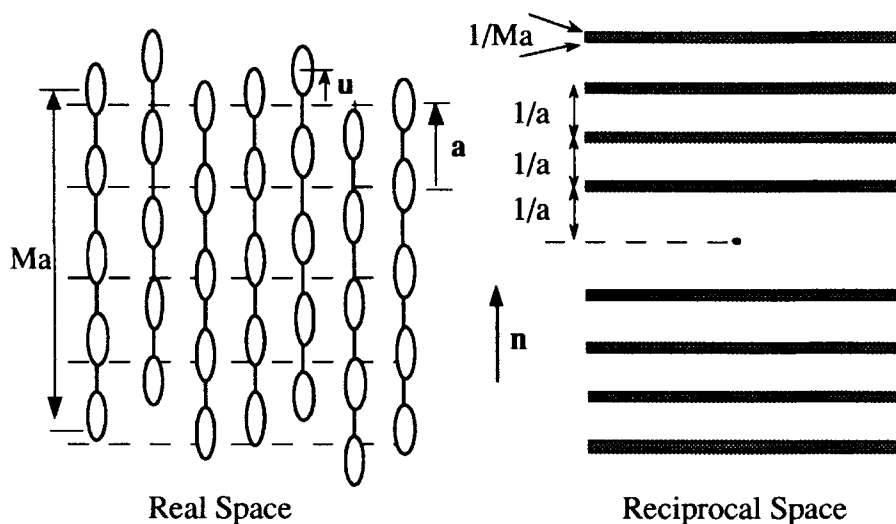


FIGURE 5 Schematic representation of the structure and diffraction pattern for a system of uncorrelated rods (uncorrelated longitudinal disorder).

Finally, an approximate evaluation of the average longitudinal displacement  $u$  of the macromolecular chains was obtained by considering the following expression for the intensity of the diffuse scattering<sup>20</sup>

$$I(\mathbf{q}) = f^2 \frac{\sin^2(\mathbf{M}\mathbf{q}\cdot\mathbf{a}/2)}{\sin^2(\mathbf{q}\cdot\mathbf{a}/2)} \sin^2(\mathbf{q}\cdot\mathbf{u}) \quad (4)$$

where  $\mathbf{a}$  is the periodicity vector of the chain,  $f$  is the form factor of the repeat unit,  $\mathbf{u}$  is the displacement of the molecule out of its mean position, and  $M$  the number of molecules in the rows (see Figure 5). Equation (4) is strictly valid only for polymeric

smectic phases where a real one-dimensional lattice is present. However, its validity has been extended to the nematic order by replacing the smectic layer period with the apparent molecular length in the nematic phase, i.e.  $a=L_{\text{diff}}$ . According to Equation (1), the intensities of the diffuse streaks are proportional to  $\sin^2(\mathbf{q} \cdot \mathbf{u})$ , so that from the intensity profile of the diffuse reflections along the meridian it is possible to estimate the amplitude  $u$  of the average longitudinal displacement. Figure 6 shows the intensity profile of the diffuse reflections along the meridional line of sample TDI-C6C6 after normalization to the square of the form factor  $f$ , i.e.  $I(q)/f^2$ , where  $q$  is the projection of the scattering vector along the meridional line. The square sinusoidal modulation predicted by Equation (1) is clearly visible, as evidenced by the thin continuous line interpolating the peak intensities. From the position  $q'$  of the first zero of the interpolating function (see Figure 6), the value of  $u$  is readily obtained as  $u=\pi/q'$ . For sample TDI-C6C6 the value of  $q'=0.75$  gives  $u=4.2$  Å. Similar values were obtained within the experimental errors for the other samples.

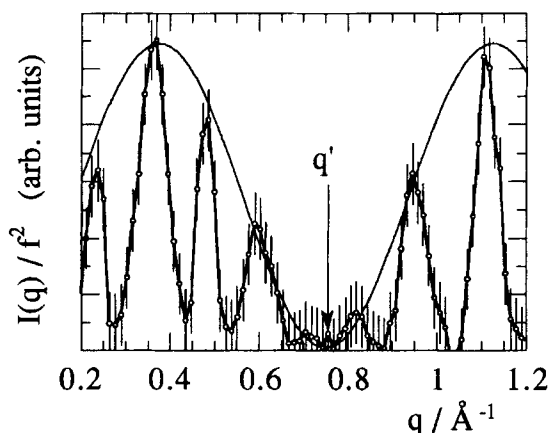


FIGURE 6 The behavior of the ratio  $I(q)/f^2$  between the intensity of the diffuse reflections along the meridian of sample TDI-C6C6 and the square of the structure factor  $f$  of the repeat unit. The thin continuous line interpolates the peak intensities.

## CONCLUSIONS

Two different molecular types of order exist within the cybotactic nematic phase to which different internal degrees of correlation correspond. The average dimension of the cybotactic groups along the director is comprised between  $\sim 260$  and  $\sim 560$  Å, whereas

the average dimension perpendicular to the director ranges from  $\sim 130$  to  $\sim 270$  Å. Accordingly, the cybotactic groups present an ellipsoidal-like shape.

By contrast, the correlation length within the nematic surrounding the cybotactic groups and along the director is comprised between 38 and 45 Å. This value is of the order of the molecular length. These findings highlight the multidomain nature of the cybotactic nematic mesophase consisting of large and asymmetric clusters even though the correlation in the surrounding nematic is very low.

The peculiar liquid crystalline behavior of the present poly(urethane-ester)s reflects a stabilizing action promoted by hydrogen bonding interactions between urethane moieties. This effect is being investigated by FT-IR spectroscopy and dynamic-mechanical measurements.

#### ACKNOWLEDGEMENT.

This work was supported from the Ministero dell'Università e della Ricerca Scientifica e Tecnologica of Italy.

#### REFERENCES

1. P.J.Stenhouse, E.M.Valles, S.W.Kantor, and W.J.McKnight, Macromolecules, **22**, 1467 (1989).
2. G.Smyth, E.M.Valles, S.K.Pollack, J.Grebowicz, P.J.Stenhouse, S.L.Hsu, and W.J.McKnight, Macromolecules, **23**, 3389 (1990).
3. R.Lorenz, M.Els, F.Haulena, A.Schmitz, and O.Lorenz, Angew. Makromol.Chem., **180**, 51 (1990).
4. W.Mormann, and M.Brahm, Macromolecules, **24**, 1096 (1991).
5. S.K.Pollack, G.Smyth, F.Papadimitrakopoulos, P.J.Stenhouse, S.L.Hsu, and W.J.McKnight, Macromolecules, **25**, 2381 (1992).
6. E. Chiellini, G. Galli, S. Trusendi, A. S. Angeloni, M. Laus, and O. Francescangeli, Mol. Cryst. Liq. Cryst., **243**, 135 (1994).
7. O. Francescangeli, B. Yang, M. Laus, A. S. Angeloni, G. Galli, and E. Chiellini, J. Polym. Sci., Polym. Phys., **33**, 699 (1995).
8. O. Francescangeli, M. Laus, G. Galli, Phys. Rev. E, in press.
9. J. B. Lee, T. Kato, T. Yoshida, and T. Uryu, Macromolecules, **26**, 4989 (1993).
10. A. Blumstein, O. Thomas, J. Asrar, P. Markis, S. B. Clough, and R.B. Blumstein, J. Polym. Sci. Polym. Lett. Ed., **22**, 13 (1984).

11. A.DeVries, Mol. Cryst. Liq. Cryst., **10**, 219 (1970).
12. P.J. Flory, Statistical Mechanics of Chain Molecules (Interscience, New York, 1969)
13. A. Guinier, X-ray Diffraction in Crystals, Imperfect Crystals and Amorphous Bodies (W.H. Freeman, San Francisco, 1963)
14. R.W.James, The Optical Principles of the Diffraction of X-Rays (Bell, London, 1948)
15. P. Davidson, P. Keller and M. Levelut, J. Phys. Paris, **46**, 939 (1985).
16. P. Davidson and M. Levelut, J. Phys. Paris, **50**, 2415 (1989).
17. F. Hardouin, S. Méry, M. F. Achard, M. Mauzac, P. Davidson, and P. Keller, Liq. Cryst., **8**, 565 (1990).
18. A. M. Levelut, Y. Fang, and C. Destrade, Liq. Cryst., **4**, 441 (1989).
19. A. De Vries, A. Ekachai, and N. Spielberg, Mol. Cryst. Liq. Cryst., **49**, 143 (1979).
20. R. Comès, M. Lambert, and A. Guinier, Acta Crystallogr., **A26**, 44, 1970.